Catal Lett (2008) 126:89–95
DOI 10.1007/s10562-008-9581-7

An Extremely Active Pt/Carbon Nano-Tube Catalyst for Selective Oxidation of CO in H_2 at Room Temperature

Ken-ichi Tanaka · Masashi Shou · Hongbin Zhang · Youzhu Yuan · Tokio Hagiwara · Atsushi Fukuoka · Junji Nakamura · Daling Lu

Received: 5 June 2008 / Accepted: 3 July 2008 / Published online: 13 August 2008

Abstract Pt catalyst supported on carbon nano-tube (CNT) was extremely active for the selective oxidation of CO in H_2 at room temperature, which was remarked contrast to the Pt supported on an active carbon (Vulcan carbon) and a graphite powder. Complete oxidation of CO was attained on a 5 wt.% Pt/CNT catalyst (0.8 g) at ca. 40 °C when the O_2/CO ratio in a flow of H_2 (20 mL/min) + CO (3.0 mL/min) + O_2 + N_2 was adjusted to be larger than 0.75 at the total flow rate of 100 mL/min. Specific activity of the Pt/CNT catalyst was explained by efficient provision of reactant molecules diffusing on CNT surface to Pt particles.

K.-i. Tanaka (✉) · M. Shou · T. Hagiwara
Advanced Science Research Laboratory, Saitama Institute of Technology, 1690 Fusaiji, Fukaya, Saitama 369-0293, Japan
e-mail: ktanaka@sit.ac.jp

H. Zhang · Y. Yuan
State Key Laboratory of Physical Chemistry of Solid Surfaces, Department of Chemistry, Xiamen University, Xiamen 361005, China

A. Fukuoka
Catalysis Research Center, Hokkaido University, Sapporo 001-0021, Japan

J. Nakamura
Graduate School of Pure and Applied Science, Tsukuba University, Tennoudai 1-1-1, sukuba, Tsukuba, Ibaraki 304-8573, Japan

D. Lu
Chemical Resources Laboratory, Tokyo Institute of Technology, 4259 Nagatsuta, Midori-ku, Yokohama 226-8503, Japan

Keywords Selective oxidation of CO · Pt/nano-tube carbon · Pt/Graphite · Pt/Vulcan carbon · CO tolerant hydrogen fuel cell

1 Introduction

Hydrogen fuel cell generates the power by the shift reaction gas is impossible at the present time, because the anode of hydrogen fuel cell is poisoned by several 10th ppm CO. Fore example, 50 ppm CO for a Pt–Ni/C anode [1] and 100 ppm CO for Pt–Ru on defect free carbon nanotube (CNT) [2]. Therefore, CO in hydrogen fuel is lowered to ca. 10 ppm by preferential oxidation (PROX) reaction using Ru catalyst at 150–170 °C. So far, several low temperature catalysts for the selective oxidation of CO in H_2 have been reported [3–9]. The mechanism of selective oxidation of CO in H_2, however, has never been clarified. Very recently, it was proved that the selective oxidation of CO on a FeOx/Pt/TiO_2 catalyst is not caused by the oxidation of HCOO intermediate with OH instead of a competitive oxidation of adsorbed CO with oxygen [10, 11].

In this paper, we developed an extremely active catalyst for the selective oxidation of CO in H_2 at room temperature, which was Pt catalyst supported on carbon nano-tube (CNT). Developed Pt/CNT catalyst has a lot of advantage in the activity, selectivity, and feasibility for preparation compared to the other low temperature catalysts so far developed. It is possible to remove the CO in fuel H_2 by inserting Pt/CNT catalyst in front of hydrogen fuel cell, so that it would be possible to operate a polymer electrolyte hydrogen fuel cell (PEFC) in H_2 containing several 1,000 ppm CO. In this paper, we discuss the amazing role of carbon nano-tubes of Pt/CNT for the oxidation of CO in

H_2 by comparing with the performance of Pt/Graphite powder and Pt/Vulcan Carbon catalysts.

2 Experimental

In the experiments, carbon nano-tubes from two different sources, CNT**(i)** and CNT**(ii)**, were used as the support. CNT**(i)** is a commercially available carbon nano-tube (Microphase Co.), and CNT**(ii)** is a multi-walled fish tail structure carbon nano-tube made from CH_4 by using Ni/MgO catalyst [12, 13]. The CNT**(ii)** takes 10–50 nm of outer-diameter and 3–7 nm of inner diameter, and elemental analysis showed about 8–10 wt.% Ni/MgO in a CNT**(ii)**. Surface area of the CNT**(i)** and the CNT**(ii)** was 114 and 140 m^2/g, respectively. Ni/MgO in CNT**(ii)** was removed in by heating CNT**(ii)** in a HNO_3 solution at 80 °C for 16 h, which was named as CNT**(ii)-p**. However, it is difficult to remove completely Ni–MgO from the CNT**(ii)-p** as shown in Fig. 1a, b. It was difficult to detect the difference of the outer surface of CNT**(ii)** and CNT**(ii)-p** by the TEM although the surface of CNT**(ii)-p** may be oxidized by heating in HNO_3 solution. The surface of CNT**(ii)** may have a lot of step edges because of its fish tail structure. To know the effect of the edges to the catalytic oxidation of CO, the activity of a 5 wt.% Pt/CNT(ii) was compared with a 5 wt.% Pt/CNT**(iii)**, where the CNT**(iii)** prepared from CO took a bamboo shape structure with low edge density.

To make clear the influence of precursor compound of Pt on the activity, catalyst was prepared by depositing Pt from three Pt-precursor compounds, $Pt(NH_3)_2(NO_2)_2$, H_2PtCl_6, and $Pt(CH_3COCHCOCH_3)_2$ on carbon nano-tubes of CNT**(i)**, CNT**(ii)** and CNT**(ii)-p**, CNT**(iii)**, Vulcan carbon (Cabot Co.) (218 m^2/g), and graphite powder.

The carbon support degassed for 2 h at room temperature was immersed in a solution of Pt-precursor compounds; a nitric acid solution of $Pt(NH_3)_2(NO_2)_2$, an aqueous solution of H_2PtCl_6, and an acetone solution of $Pt(acac)_2$ for more than 12 h. After then, vaporized the solvent in a flow of N_2 at 40 °C and subjected to the reduction with H_2 at 200 °C. Catalytic reaction was performed by flowing a mixture of $O_2 + CO + H_2 + N_2$ through a fixed bed catalyst in a Pyrex glass reactor, where O_2/CO ratio was adjusted to be 1/2 (stoichiometric ratio) or 1/1. A steady conversion attained by flowing a mixture gas for more than 30 min at each reaction temperature. Conversion was evaluated from the CO and O_2 analyzed by an on-line gas chromatography with a molecular sieve column.

3 Results and Discussion

Figure 2a shows the conversion of CO and O_2 attained by flowing a mixture of CO (1.5 mL/min) + O_2 (1.5 mL/min) + H_2 (15.0 mL/min) + N_2 (42.0 mL/min) on 15 wt.% Pt catalysts supported on three different carbon

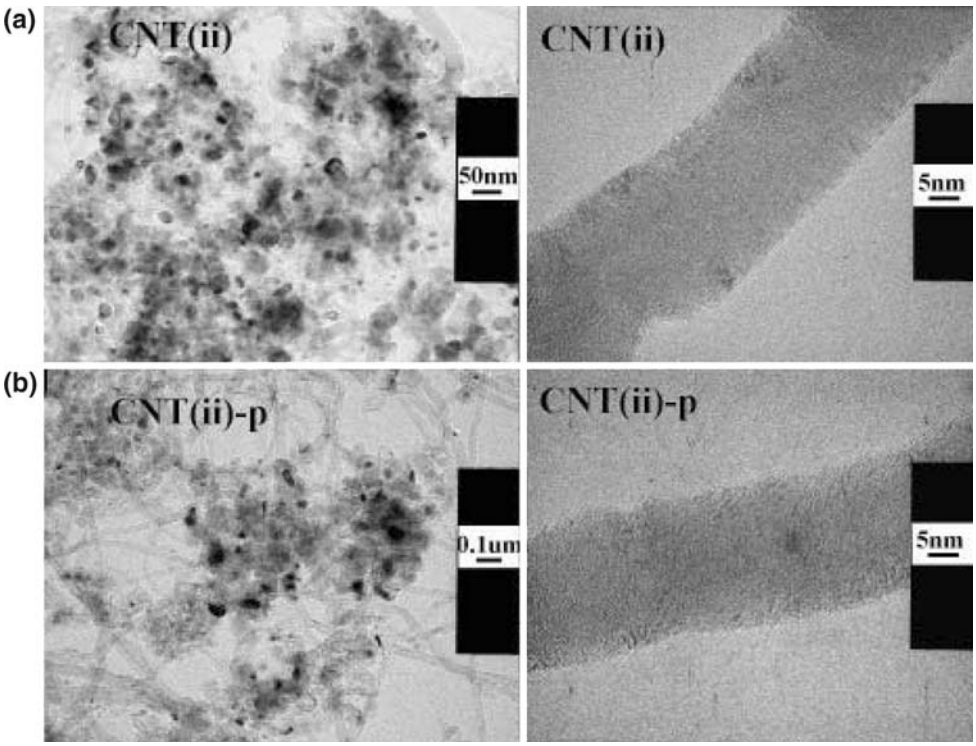

Fig. 1 TEM image of (**a**) CNT**(ii)** and (**b**) CNT**(ii)-p**. Ni/MgO are remained in CNT**(ii)-p** as seen the dark dots

supports, Pt/CNT**(i)** (0.39 g), Pt/Vulcan Carbon (0.34 g) and Pt/Graphite (0.8 g). 15 wt.% Pt was deposed from $Pt(NH_3)_2(NO_2)_2$ precursor. It is known that the Pt/CNT**(i)** is exceptionally active giving ca. 100% conversion of CO and O_2 at 40 °C, where the conversion of CO does not indicate the selectivity because the ratio of O_2/CO is 1/1.

About 15 wt.% Pt/Vulcan-C and 15 wt.% Pt/Graphite are clearly less active compared to 15 wt.% Pt/CNT**(i)** at 40 °C although the Pt particles observed in the TEM images in Fig. 2 seem to take similar size on the three catalysts. In fact, the particle size decided by the XRD peak width (not shown here) was 4.0–4.5 nm for the Pt/CNT**(i)**, and 3.0–4.5 nm for the Pt/Vulcan-C. Therefore, we conclude that the size of dispersed Pt particles is not responsible for superior activity of the Pt/CNT**(i)** catalyst To investigate the influence of precursor Pt compound used to deposit Pt, a 15 wt.% Pt/CNT**(i)** catalyst prepared from

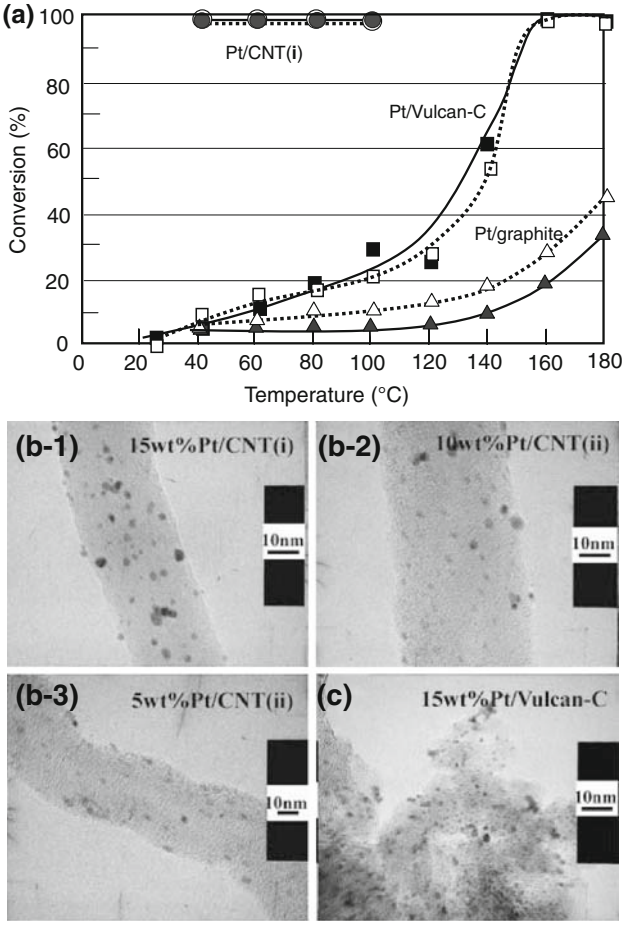

Fig. 2 (**a**) Conversion of CO (solid) and O_2 (open) in a flow of CO (1.5 mL/min) + O_2 (1.5 mL/min) + H_2 (15.0 mL/min) + N_2 (42.0 mL/min) on 15 wt.% Pt/CNT**(i)** (●, ○) (0.39 g), 15 wt.% Pt/Vulcan-C (■, □) (0.34 g), and 15 wt.% Pt/Graphite (▲, △) (0.8 g) catalysts. The TEM images are 15 wt.% Pt/CNT**(i)** (**b-1**), 10 wt.% Pt/CNT**(ii)** (**b-2**), 5 wt.% Pt/CNT**(ii)** (**b-3**), and (**c**) 15 wt.% Pt/Vulcan-C, where Pt was deposited from $Pt(NH_3)_2(NO_2)_2$ precursor

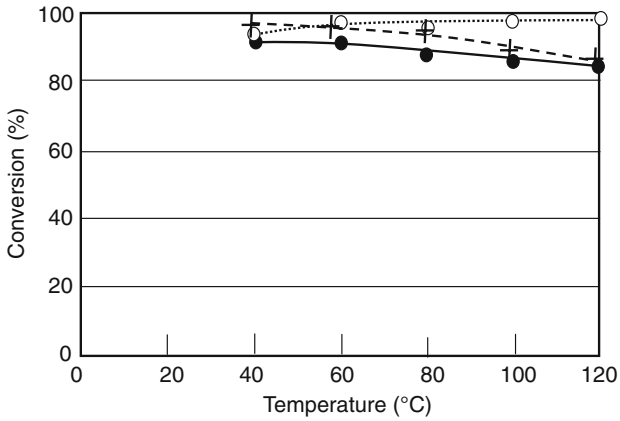

Fig. 3 Conversion of CO (●) and O_2 (○) in a flow of a mixture of CO (3.0 mL/min) + O_2 (1.5 mL/min) + H_2 (20.0 mL/min) + N_2 (75.5 mL/min) on 15 wt.% Pt/CNT**(i)** (0.8 g) catalyst prepared from H_2PtCl_6 precursor. (+) indicates the selectivity

H_2PtCl_6 was studied. The Pt/CNT**(i)** catalyst was also active as shown in Fig. 3, where the reaction was performed by flowing a mixture of CO (3.0 mL/min) + O_2 (1.5 mL/min) + H_2 (20.0 mL/min) + N_2 (75.5 mL/min). The ratio of O_2/CO in the flow gas was 1/2, so the CO conversion at ca. 95% conversion of O_2 indicates high selectivity (>90%) for the oxidation of CO in H_2 at temperature lower than 80 °C.

We found the deposition of Pt on CNT from $Pt(acac)_2$ complex gave large Pt particles, which took 13–15 nm on the n-tube-C**(i)** and 9.0–11 nm on the Vulcan-C by XRD analysis. These sizes are in good agreement with the TEM images shown in Fig. 4b, c. Catalytic activity of the Pt/CNT**(i)** and Pt/Vulcan-C catalysts prepared from $Pt(acac)_2$ were undoubtedly less active compared to the Pt/CNT**(i)** and Pt/Vulcan-C prepared from $Pt(NH_3)_2(NO_2)_2$ as shown in Fig. 4a. It is note worthy fact that if we compare the activity of Pt/CNT**(i)** to that of Pt/Vulcan-C, the Pt/CNT clearly gives higher activity than the Pt/Vulcan-C although the Pt particles on Vulcan-C are smaller than those on the CNT.

It is reasonable to speculate that the Pt may take similar electronic state on CNT and graphite, and may be on Vulcan carbon too. Therefore, we considered that the CNT surface plays an essential role to promote the catalytic oxidation of CO in H_2 on Pt particles. To shed light on this question, we compared the activity of 5 wt.% Pt supported on the CNT from different sources, which were CNT**(ii)**, CNT**(ii)-p**, and CNT**(iii)**. As described in the experimental section, the CNT**(ii)** was made from CH_4 but the CNT**(ii)** was made from CO. Conversion of CO and O_2 attained on the 5 wt.% Pt/CNT**(ii)** (0.8 g), the 5 wt.% Pt/CNT**(ii)-p** (0.8 g), and 5 wt.% Pt/CNT**(iii)** are shown in Fig. 5a–c. It is known that both the Pt/CNT**(ii)** and the Pt/CNT**(iii)** catalysts are extremely active at low temperature, but the

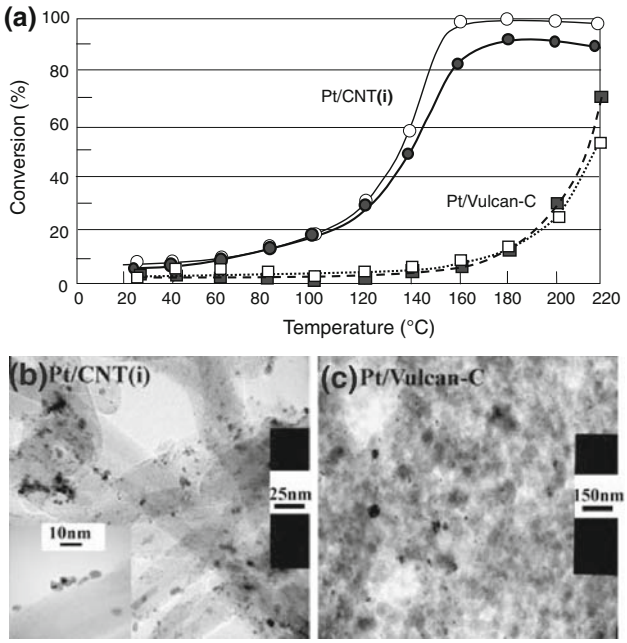

Fig. 4 (**a**) Conversion of CO (●, ■) and O_2 (○, □) in a flow of CO (1.5 mL/min) + O_2 (1.5 mL/min) + H_2 (15 mL/min) + N_2 (42.0 mL/min) on 15 wt.% Pt/CNT(**i**) (0.39 g) and 15 wt.% Pt/Vulcan-C (0.29 g) prepared from $Pt(acac)_2$ precursor. TEM images indicate relatively large particles in (**b**) 15 wt.%Pt/CNT(**i**) and in (**c**) 15 wt.% Pt/Vulcan-C

activity of the Pt/CNT(**ii**)-**p** is low, which is similar to that of the 15 wt.% Pt/Vulcan-**C** (broken line). It is also worthy of note that the particle size of Pt on CNT does not change by increasing the amount of Pt on the CNT as shown in Fig. 2 b-1–b-3, and no difference of the size of Pt particles was observed between Pt/CNT(**ii**) and Pt/CNI(**ii**)-**p** as shown in Fig. 5. However, the activity is quite different between Pt/CNT(**ii**) and Pt/CNI(**ii**)-**p**. We have to remind that CNI(**ii**)-**p** was heated in a HNO_3 solution to remove the Ni–MgO catalyst, but the Ni–MgO was not completely removed. Taking these facts into account, the role of Ni–MgO contained in CNT(**ii**) and CNT(**ii**)-**p** is riddle at the present time.

Figure 6 shows the conversion of CO in H_2 increased with the ratio of O_2/CO on the 5 wt.% Pt/CNT(**ii**) at room temperature. It is known that the complete oxidation of CO is attained at the ratio of O_2/CO = 0.75. Almost equal O_2/CO ratio was confirmed for the complete oxidation of CO on the 5 wt.% Pt/CNT(**i**) catalyst, too. Taking these results into account, the complete oxidation of 2,000 ppm CO (<0.2 ppm) in H_2 with 2,000 ppm O_2 was confirmed over a 10 wt.% Pt/CNT(**i**) catalyst (0.19 g) at room temperature by flowing H_2 at 100 mL/min for more than 20 h [10]. Accordingly, we conclude that the Pt/CNT catalysts are not only active at low temperature but have superior selectivity compared to the conventional Ru catalyst (O_2/CO = 1.0–1.5).

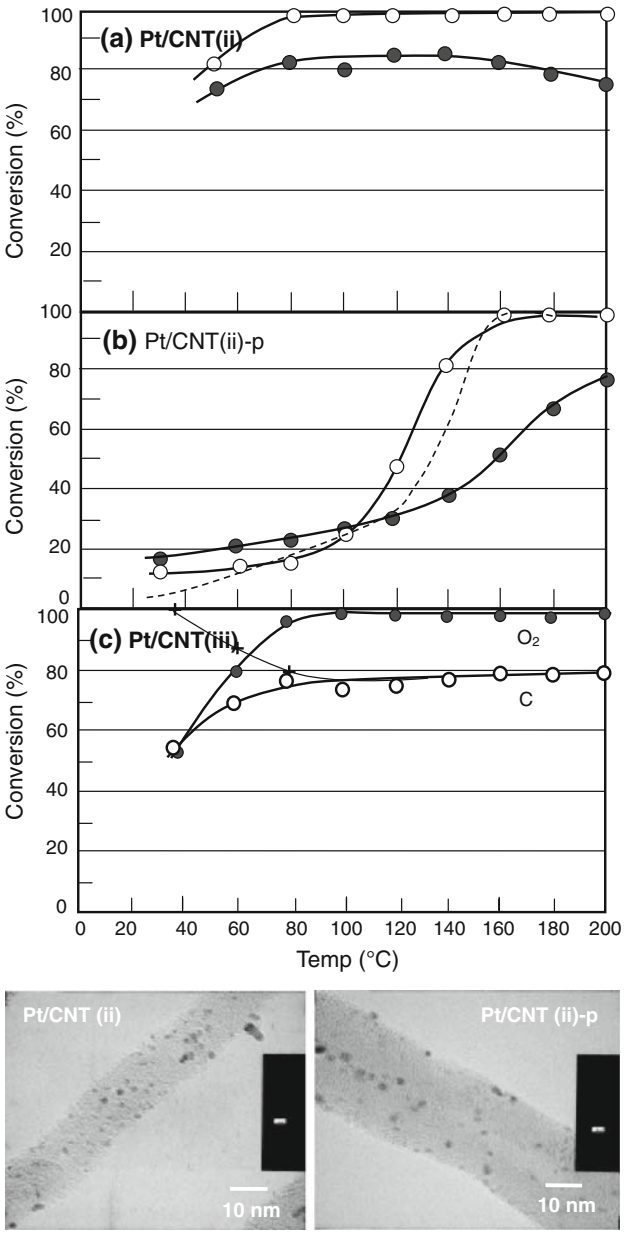

Fig. 5 Conversions of CO (●) and O_2 (○) in a flow of CO (3.0 mL/min) + O_2 (1.5 mL/min) + H_2 (20 mL/min) + N_2 (75.5 mL/min) on 5 wt.% Pt/CNT(**ii**) with Ni–MgO (0.8 g) (**a**), on 5 wt.% Pt/CNT(**ii**)-**p** removed Ni–MgO (0.8 g) (**b**), and on 5 wt.% Pt/CNT(**iii**) made from CO (0.8 g) (**c**). A broken line in (**c**) indicates the approximate activity of 15 wt.% Pt/Vulcan-C catalyst. TEM images are the 5 wt.% Pt/CNT(**ii**) and the Pt/CNT(**ii**)-**p**

It is reasonable speculation that the electronic state of Pt particles is similar on CNT and graphite, but the catalytic activity of these two is quite different. One unique feature of CNT is its closed surface with nano-meter size diameter, and the CNT(**ii**) made from CH_4 has a fish tail structure having a lot of edges. The dynamics of reactant molecules weakly adsorbed on a closed nano-tube surface may be different from that on the graphite with open surface, that

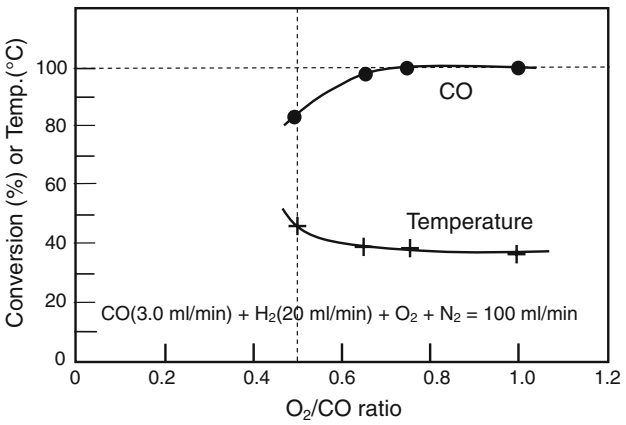

Fig. 6 The conversion of CO (●) increasing as the ratio of O_2/CO on the 5 wt.% Pt/CNT**(ii)** catalyst (0.8 g) at 35–40 °C, where the total flow rate was 100 mL/min of a mixture of H_2 (20 mL/min) + CO (3.0 mL/min) + O_2 + N_2

is, molecules will take a quasi-one dimensional motion along the tube axis on the CNT as illustrated in Fig. 7d. In this meaning, we could say that the motion of adsorbed molecule on a closed surface such as C_{60} and C_{70} will be a quasi-zero dimensional because the molecule necessarily returns to its starting position.

We wish to point out an interesting role of the support surface but has been ignored in catalysis, that is the transportation of molecules to active particles or to active sites through the support surface. We could say that the phenomena in heterogeneous systems do not proceed efficiently without the contribution of inactive surface area, which is the feature of heterogeneous systems. For example, transformation of molecules or atoms over the inactive area is indispensable to the rapid growth of crystals, the effective growth of the steps, and the rapid reaction in enzyme. So far the selectivity in heterogeneous catalysis

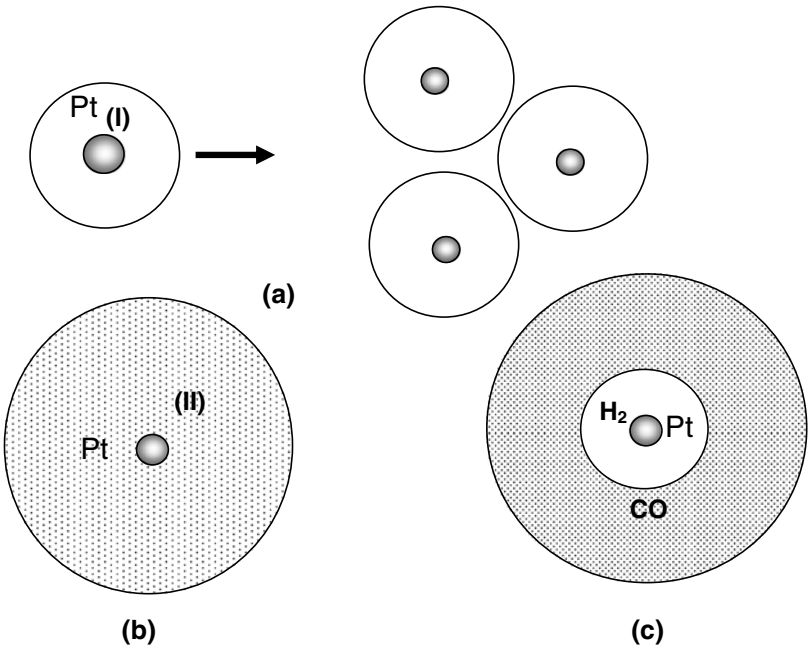

Activity of Pt depends on diffusion territory providing molecules

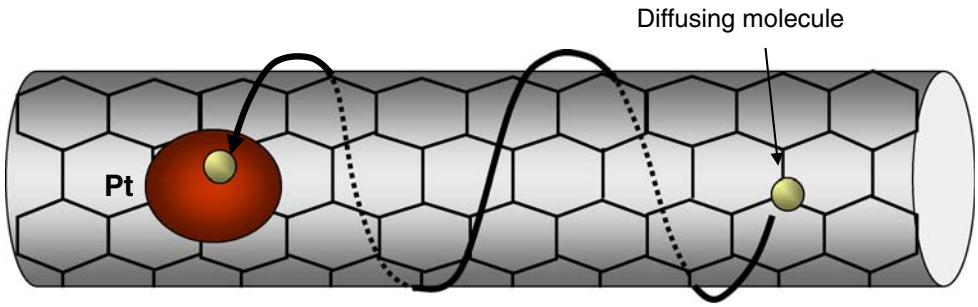

(d) Quasi-one dimensional migration of molecule to a Pt particle.

Fig. 7 Reactant molecules provide to Pt through support surface. (**a**) When one particle disperses into three particles, contributable support surface becomes three times. (**b**) When two molecules (a) and (b) have different diffusion length on the support, Pt prefers molecules having longer diffusion length. (**c**) If CO has longer diffusion length (gray area) than H_2 (white area) on carbon nano-tube surface, preferential oxidation of CO may take place. (**d**) Quasi-one dimensional transportation on a closed nano-tube surface

has been explained by the kinetics based on the competitive adsorption or competitive reaction on active sites or active particles, that is, one premises the adsorption of molecules by direct collision on these active surface or sites. If the reactant molecules on Pt are predominantly supplied by the migration over the support CNT surface, the activity as well as the selectivity of Pt will be controlled by migration length of molecules on the support. As illustrated in Fig. 7, longer the migration length on support provides larger contributable support area to the reaction on Pt. In other word, the sticking probability or the reaction probability of molecules depends on the contributable territory of the support surrounding a Pt particle, so that the longer the migration length, the higher the sticking probability or the reaction rate on Pt. From this idea, we could speculate a specific feature of nano-tube surface, on which migration of molecule would be quasi-one dimensional so that migrating molecules will encounter Pt particles more efficiently than that on the open surface like graphite.

We have to say that it is difficult to detect the two-dimensional gas like molecules on the support being in equilibrium with gas phase. However, when the adsorption is not in equilibrium with gas phase, we can deduce the contribution of precursor state in adsorption. Adsorption of CH_3OH or C_2H_5OH on Si(111)-7 $\times$ 7 surface is a typical example, where an alcohol (ROH) molecule dissociates on a pair site of Si-adatom and Si-rest atom into RO–Si-adatom and H–Si-rest atom [14, 15]. Interesting fact was that the dissociation proceeded with a constant sticking probability until saturation although available dissociation sites decreased as increasing the adsorption. It is clear that few molecules dissociate by direct collision with vacant pair sites, and predominant molecules are provided by diffusing over the inactive area with saturated sites. This phenomenon suggests that the inactive surface area contributes to the efficient dissociation of alcohol at the active sites, which is a good model suggesting a relation between the active metals on inactive support surface.

If CO and H_2 adsorb on Pt via precursor state adsorption on the CNT surface, the oxidation rate of CO and H_2 depends on the diffusion territory surrounding Pt particles on the CNT, because wider territory surrounding a Pt particle will provide more molecules to Pt. If this mechanism would be acceptable, higher the activity will give higher the selectivity as illustrated in Fig. 7c, and the preferential oxidation of CO on the Pt/CNT catalyst is perhaps this case. That is, the preferential oxidation of CO on the Pt/CNT catalyst suggests longer migration path of CO than that of H_2 This is clearly different from our knowledge premising competitive adsorption and reaction kinetics, which suggests higher the selectivity lowers the activity.

When a Pt particle (r_o) disperses into small particles (r), the activity will change according to $1/\rho^n$, where $\rho = r/r_0$. When the whole spherical metal surface is active and dispersed particles take sphere shape, the activity will increase according to the 1st order with respect to $1/\rho^n$. If metal particles have attractive interaction with support surface, dispersed metal particles will be flat. In this case, the activity changes little by the dispersion because it changes in the zero order with respect to $1/\rho^n$. On the other hand, when perimeter of the particle is active, the activity will increase according to the 2nd order with respect to $1/\rho^n$. In contrast, when the support surface contributes to the reaction, the activity will increase according to the 3rd order with respect to $1/\rho^n$. Unfortunately, it is difficult to adjust the size of Pt particles on CNT, we could not confirm the order (n) of $1/\rho^n$ at the present time. However, an interesting example can be found on the activity of Au particles depending on the size. Although Haruta [16] assumed the active perimeter for the Au particles, but the activity is undoubtedly increased higher than the 2nd order with respect to particle size as shown in Fig. 8. In this figure, three curves of $1/\rho^n$ ($n = 1, 2, 3$) are described.

Finally, we mention the effect of H_2 and H_2O on the oxidation of CO on Pt/CNT, because H_2 or H_2O markedly enhanced the oxidation of CO on our previously developed $FeOx/Pt/TiO_2$ catalyst. We confirmed that the oxidation of CO with O_2 on Pt/CNT catalyst was also enhanced by H_2 and H_2O (added about 10 Torr (ca. 1.5%) of H_2O at room temperature). We also observed a hydrogen isotope effect on the oxidation of CO by H_2/D_2, but the mechanism of the oxidation of CO on CNT should be discussed more carefully elsewhere.

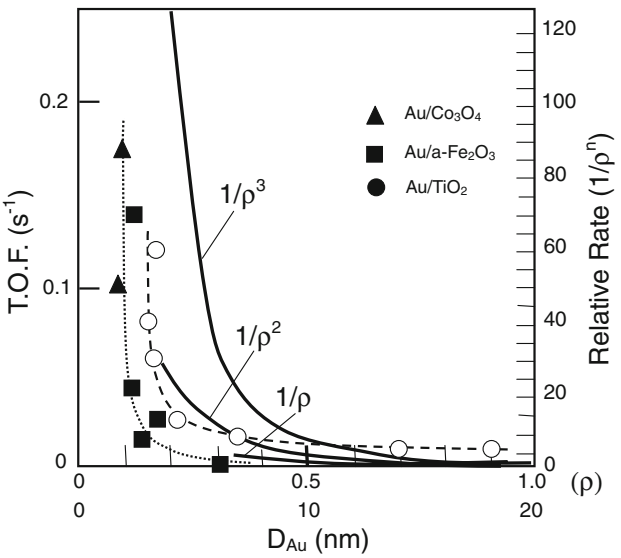

Fig. 8 Catalytic activity of Au particles increasing as decreasing their particle size [16]. Solid lines indicate the order of rate increased according to $1/\rho^n$ when the size of particles decreased from r_o to r ($\rho = r/r_0$). The value of n relates to the active part or participate part of the catalyst as described in the text

Acknowledgments Authors appreciate Kawaken Co. and Tanaka Kikinzoku Co. for their support of this work. K. Tanaka would like to express his great acknowledgement to Mr. Mitsushi Umino of Astech Co. for his long time encouragement.

References

1. Okada T, Yano H, Ono C (2007) J New Mater Electrochem Syst 10:129
2. Yoo E, Okada T, Kizuka T, Nakamura J (2007) Electrochemistry 75:146
3. Landon P, Forguson J, Solsona BE, Garcia T, Carley AF, Herzing AA, Kiely CJ, Golunski SE, Hutchings GJ (2005) Chem Comm 3385
4. Okumur M, Nakamura S, Tsubota S, Nakamura T, Azuma M, Haruta M (1998) Catal Lett 52:53
5. Bolinger MA, Vannice MA (1996) Appl Catal B, Environ 8:417
6. Shou M, Tanaka K, Yoshioka K, Moro-oka Y, Nagano S (2004) Catal Today 90:255
7. Tanaka K, Moro-oka Y, Ishigure K, Yajima T, Okabe Y, Kato Y, Hamano H, Sekiya S, Tanaka H, Matsumoto Y, Koinuma H, He Hong, Zhang C, Feng Q (2004) Catal Lett 92:115
8. Shi X, Zhang C, Shou M, He H, Sugihara S, Tanaka K (2006) Catal Lett 107:1
9. Fukuoka A, Kimura J, Oshio T, Sakamoto Y, Ichikawa M (2007) J Am Chem Soc 33:10120
10. Shi X, Tanaka K, He H, Shou M, Xu W, Zhang X (2008) Catal Lett 120:210
11. Tanaka K, He H, Shi X, Shou M, Zhang X, Ito M submitted
12. Chen P, Zhang HB, Lin GD, Hong Q, Tsai KR (1997) Carbon 35:1495
13. Zhang HB, Lin GD, Zhou QZH, Dong X, Chen T (2002) Carbon 40(13):2429
14. Xie Z-X, Uematsu Y, Lu Xin, Tanaka K (2002) Phys Rev B 66:125306
15. Liu H-J, Xie Z-X, Watanabe H, Qu J, Tanaka K (2006) Phys Rev B 73:165421
16. Haruta M (1997) Catal Today 35:153